

A SPECIFIC MAGNITUDE BUDGET FOR THE DETECTION OF 36 NUCLEAR EARTHQUAKES NEAR LARGE URBAN AREAS SUBJECT TO A NATURAL SEISMIC HAZARD.

ALEXIS ZAGANIDIS

ABSTRACT. Multiple underground nuclear explosions may trigger the rupture of seismic faults and mimic a natural earthquake. Moreover, multiple nuclear explosions can be spatially arranged (on a vertical line for instance) and temporally synchronized in order to reduce significantly the P-waves (except inside both spherical cones along the vertical line arrangement).

A Specific Magnitude Budget, with the relevant elementary approximations, is relatively enough accurate to compare unambiguously the energy of the stress drop over the fault rupture and the energy of the radiated seismic waves.

Indeed, for the largest natural earthquakes precisely recorded ($6.9 \leq M_w \leq 7.3$), we define very conservatively their average seismic radiation efficiency to 0.25. It follows from that definition, the natural seismic radiation efficiency ranges between 0.113 and 0.520 around the average 0.269 (the natural Specific Magnitude Budget range between $\Delta_{nat}^{min} M_Z = -0.630$ and $\Delta_{nat}^{max} M_Z = -0.189$ around the average $\Delta_{nat}^{mean} M_Z = -0.380$).

On the other hand, the nuclear seismic radiation efficiency ranges between 1.185 and 1.113 around the average 81.9 (the nuclear Specific Magnitude Budget range between $\Delta_{nuc}^{min} M_Z = 0.049$ and $\Delta_{nuc}^{max} M_Z = 2.031$ around the average $\Delta_{nuc}^{mean} M_Z = 1.275$).

In practice, the natural seismic radiation efficiency is always $2.278\times$ times smaller than the nuclear seismic radiation efficiency (an artificial gap of the Specific Magnitude Budget $\Delta_{gap} M_Z = 0.238$ is found). Indeed, to provoke a more powerful stress drop over the fault rupture with multiple underground explosions, an accurate information about the future epicenters should be known which is impossible in practice. Lowering too much the energy of the multiple underground nuclear explosions would also increase the risk of not triggering at all the rupture of a seismic fault.

A Specific Magnitude Budget for the detection of 32 giant nuclear earthquakes near large urban areas subject to an existing Natural Seismic Hazard is an extremely important research task to do for the nuclear safety of the world (nuclear explosions could be spatially arranged and temporally synchronized to reduce the P-waves and to trigger the rupture of the existing seismic faults).

Elementary approximations in the well established framework of the propagating waves in continuous media are used for the Specific Magnitude Budget in the present article.

- 1- The Kinetic energy of the propagating waves in continuous media is roughly equal to the Potential energy of that ones.
- 2- If the seismic station is not far away from the seismic wave source ($\sqrt{x^2 + y^2} < 4 \times h$), the seismic waves come directly from the source itself. The Specific Energy & Magnitude Budget with this previous hypothesis are the following:

$$\begin{aligned}
 R_Z &= E_R/E_{Work} \\
 &= \frac{12\pi}{64} \times C_Z \times \rho \times \overline{PGV}^2 \times d_e^2 \times V_S \times \Delta T_S/E_{7.0} \\
 (1) \quad &\times \exp(\bar{\alpha}_S \times d_e / \log(31.62, e)) / 31.62^{0.898 \times (M_w - 7.0)} \\
 \Delta M_Z &= \log(E_R) - \log(E_{Work}) \\
 (2) \quad &= \log\left(31.62, \frac{12\pi}{64} \times C_Z \times \rho \times \overline{PGV}^2 \times d_e^2 \times V_S \times \Delta T_S/E_{7.0}\right) \\
 &\quad + \bar{\alpha}_S \times d_e - 0.898 \times (M_w - 7.0) \\
 (3)
 \end{aligned}$$

where :

$$\begin{aligned}
 (4) \quad C_Z &\cong 1/18.414 \\
 (5) \quad \rho &\cong 2\,650 \text{ kg/m}^2 & V_S &\cong 4\,500 \text{ m/s}^2 \\
 (6) \quad E_{7.0} &\cong 1.995 \times 10^{15} \text{ J} & \bar{\alpha}_S &\cong \log(31.62, e) \frac{2\pi \times \bar{f}_S}{Q_S \times V_S} \\
 (7) \quad \bar{f}_S &\cong 2 \text{ Hz} & Q_S &\cong 250
 \end{aligned}$$

The factor 4π is the unit sphere surface. The factor $3/64$ come from a doubled amplitude of the seismic waves when they reflect to the Earth's surface (factor $1/2^2$), a \sin^2 main envelop for the ground velocity (factor $3/8$) and a sinusoidal oscillation of the seismic wave (factor $1/2$).

C_Z is a universal constant for every earthquakes. \overline{PGV} is the maximum of the main envelop of the ground velocity at the seismic station. d_e is the effective hypocentral distance depending on the eccentricity of the ellipsoidal isoseisms of the Shake Map ($d_e = \sqrt{x^2 + y^2 + h^2}$ for a null eccentricity of the ellipsoidal isoseisms of the Shake Map).

ρ is the density of the rocks at the recording seismic station. V_S is the speed of the S-waves at the recording seismic station. ΔT_S is the time duration of the main envelop of the S-waves. $E_{7.0}$ is the mechanical energy of a M_w 7.0 earthquake or the mechanical energy of a M_{Work} 6.284 earthquake. \bar{f}_S is the most representative frequency of the S-Waves. Q_S is the maximal quality factor of the S-waves through the seismic attenuation.

$$(8) \quad x_h = x/h$$

$$y_h = y/h$$

$$(9) \quad l_h = l/h$$

$$(10) \quad f(x_h, y_h, l_h) = \frac{1}{l_h} \int_{-l_h/2}^{+l_h/2} \frac{dx'_h}{(x_h - x'_h)^2 + y_h^2 + 1}$$

$$(11) \quad 1/\sqrt{1-e^2} = \frac{a}{b} = \frac{\partial_y^2 f(0, 0, l_h)}{\partial_x^2 f(0, 0, l_h)}$$

$$(12) \quad d_e = \frac{h}{\sqrt{f(x_h, y_h, l_h)}}$$

x, y, h, l are the coordinates of the seismic station with respect to the isoseisms orientations, the hypocentral depth and the horizontal length of the fault rupture. a, b are the ellipse parameters of the ellipsoidal isoseisms. The equation 11 is used to derive the fault rupture ratio l/h from the ellipsoidal isoseism ratio a/b .

We define the mechanical magnitude M_{Work} of the stress drop over the fault rupture. It is closely related to the moment magnitude scale M_w as the following (Figure 1):

$$(13) \quad \begin{aligned} E_{Work} &= \frac{\Delta\sigma\mu\bar{u}S}{G} \\ &= \frac{\Delta\sigma M_0}{G} \\ &\cong \frac{\beta (SR)^{-0.23} M_0}{G} \\ &\cong \frac{\gamma \times 10^{-0.23 \times M_w / 1.5} \times 10^{1.5 \times M_w}}{G} \end{aligned}$$

$$(14) \quad \begin{aligned} 10^{1.5 \times M_{Work} + C_0} &\cong 10^{-0.23 \times M_w / 1.5 + 1.5 \times M_w + C_0} \\ M_{Work} &\cong 0.898 \times M_w \pm 0.153 \end{aligned}$$

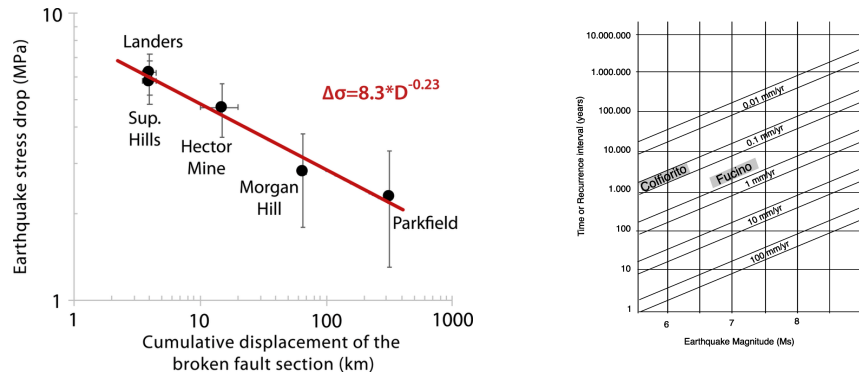


FIGURE 1

- 3- If the seismic station is far away from the seismic wave source ($\sqrt{x^2 + y^2} > 4 \times h$), the seismic waves are guided between the Earth's surface and the deeper layers of the Earth's crust. We neglect the seismic waves with an upward angle larger than 45 and with a downward angle smaller than 0 because of a much larger seismic attenuation. The Specific Energy & Magnitude Budget with this previous hypothesis are the following :

$$\begin{aligned}
R_Z &= E_R/E_{Work} \\
&= \frac{12\pi\sqrt{2}}{64(\sqrt{2}-1)} \times C_Z \times \rho \times \overline{PGV}^2 \times d_e \times h \times V_S \times \Delta T_S/E_{7.0} \\
(15) \quad &\times \exp(\bar{\alpha}_S \times d_e/\cos(\pi/8)/\log(31.62, e))/31.62^{0.898 \times (M_w - 7.0)} \\
\Delta M_Z &= \log(E_R) - \log(E_{Work}) \\
(16) \quad &= \log\left(31.62, \frac{12\pi\sqrt{2}}{64(\sqrt{2}-1)} \times C_Z \times \rho \times \overline{PGV}^2 \times d_e \times h \times V_S \times \Delta T_S/E_{7.0}\right) \\
&+ \bar{\alpha}_S \times d_e/\cos(\pi/8) - 0.898 \times (M_w - 7.0) \\
(17)
\end{aligned}$$

where :

$$\begin{aligned}
(18) \quad C_Z &\cong 1/18.414 \\
(19) \quad \rho &\cong 2\,650 \text{ kg/m}^2 & V_S &\cong 4\,500 \text{ m/s}^2 \\
(20) \quad E_{7.0} &\cong 1.995 \times 10^{15} \text{ J} & \bar{\alpha}_S &\cong \log(31.62, e) \frac{2\pi \times \bar{f}_S}{Q_S \times V_S} \\
(21) \quad \bar{f}_S &\cong 2 \text{ Hz} & Q_S &\cong 250
\end{aligned}$$

The factor $\sqrt{2}/(\sqrt{2}-1)(h/d_e)$ is the ratio between the cylinder surface of radius d_e and height h and the cone surface with the angle lying between 0 and +45. For the seismic attenuation, we used the approximate average length path $d_e/\cos(\pi/8)$ with an upward angle of +22.5.

- 4- We also used a fitted model for the \overline{PGV} with respect to the \overline{PGA} (Figures 1, 2 and 3).

Wikipedia provide the list of the costliest earthquakes. We add to that list, the earthquakes in San Fernando 1971, in Coalinga 1983, in Borah Peak 1983, in Whittier Narrows 1987, in Landers 1992, in Kushiuro 1993, in Geiyo 2001, in Southern Peru 2001, in Kaohsiung 2010, in Chiapas 2017, in Ridgecrest 2019 and in Taitung 2022. We removed from the costliest earthquake list, the earthquakes too far from a reliable recording seismic station. The earthquakes in Tangshan 1976 and in San Francisco 1906 have a great historical importance but there are no reliable recording seismic station close to both earthquakes. Therefore, we study separately the earthquake in Tangshan 1976 and the earthquake in San Francisco 1906.

We googled "location name + year + ground acceleration" to get the FULL ground acceleration plots of the earthquake. We googled "seismic station name + country

SHAKING	Not felt	Weak	Light	Moderate	Strong	Very strong	Severe	Violent	Extreme
DAMAGE	None	None	None	Very light	Light	Moderate	Moderate/heavy	Heavy	Very heavy
PGA(%g)	<0.05	0.3	2.76	6.2	11.5	21.5	40.1	74.7	>139
PGV(cm/s)	<0.02	0.13	1.41	4.65	9.64	20	41.4	85.8	>178
INTENSITY	I	II-III	IV	V	VI	VII	VIII	IX	X+

Scale based on Worden et al. (2012) Version 1: Processed 2020-02-06T19:31:16Z
 △ Seismic Instrument ○ Reported Intensity ★ Epicenter □ Rupture

PERCEIVED SHAKING	Not felt	Weak	Light	Moderate	Strong	Very strong	Severe	Violent	Extreme
POTENTIAL DAMAGE	none	none	none	Very light	Light	Moderate	Moderate/Heavy	Heavy	Very Heavy
PEAK ACC (%g)	<.17	.17-1.4	1.4-3.9	3.9-9.2	9.2-18	18-34	34-65	65-124	>124
PEAK VEL (cm/s)	<0.1	0.1-1.1	1.1-3.4	3.4-8.1	8.1-16	16-31	31-60	60-116	>116
INSTRUMENTAL INTENSITY	I	II-III	IV	V	VI	VII	VIII	IX	X+

FIGURE 2. MMI Legend of Shake Maps.

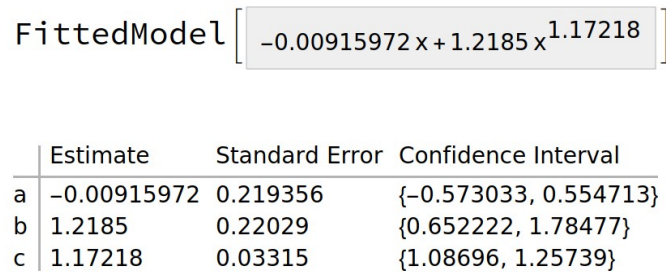


FIGURE 3. Estimate, Standard Error and Confidence Interval of the Fitted Model's Parameters for the \overline{PGV} with respect to the \overline{PGA} .

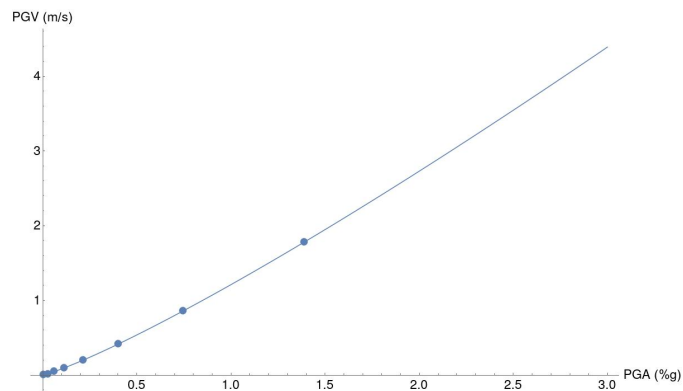


FIGURE 4. Plot of the Fitted Model for the \overline{PGV} with respect to the \overline{PGA} .

+ latitude + longitude” to get the latitude and the longitude of the recording seismic stations which have produced the ground acceleration plots found previously. The mechanical magnitude of the stress drop over the fault rupture (M_{Work}), the hypocentral depth, the GPS coordinates of the epicenter, the UTC, the local time

and the Shaking Map are given by the corresponding Wikipedia pages.

Very conservatively, we define the Specific Magnitude Budget ΔM_Z as the following:

$$(22) \quad \Delta M_Z = \log(31.62, E_R/E_{Work}) - \log\left(31.62, \langle E_R/E_{Work} \rangle_{\text{natural}}^{6.9 \leq M_w \leq 7.3}\right)$$

where

$$(23) \quad \langle E_R/E_{Work} \rangle_{\text{natural}}^{6.9 \leq M_w \leq 7.3} := 0.25$$

It may be the most useful scientific discovery: differentiating unambiguously the nuclear earthquakes to the natural earthquakes with a Specific Magnitude Budget ΔM_Z (Figure 5, 6 and 7). It was not expected being discovered so late.

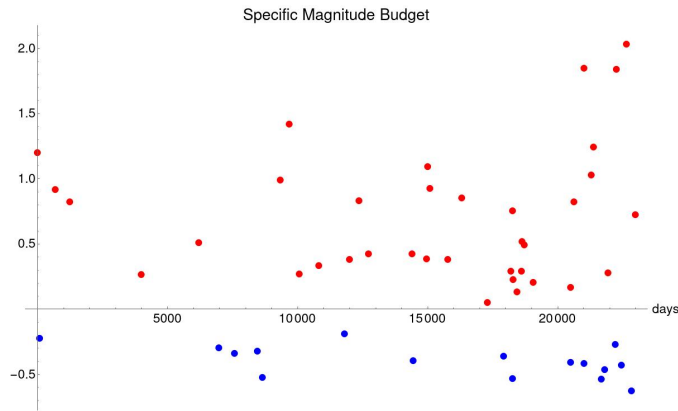


FIGURE 5. The abscissa is the number of days of the earthquakes from the first nuclear earthquake in Agadir 1960.

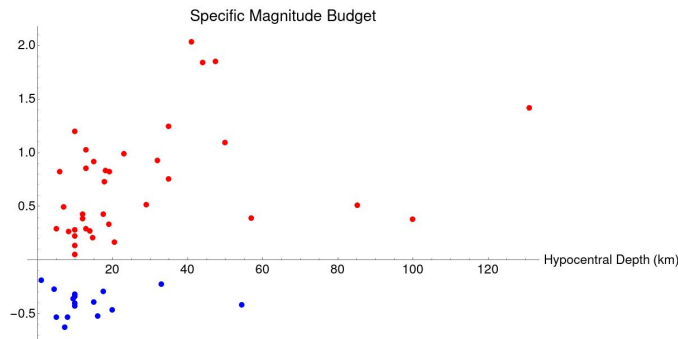


FIGURE 6

Multiple underground nuclear explosions may trigger the rupture of seismic faults and mimic a natural earthquake. Moreover, multiple nuclear explosions can be

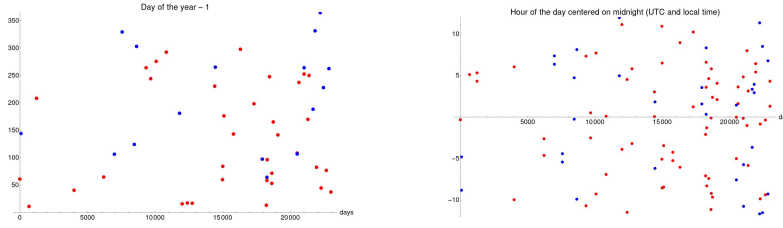


FIGURE 7. The abscissa is the number of days of the earthquakes from the first nuclear earthquake in Agadir 1960.

spatially arranged (on a vertical line for instance) and temporally synchronized in order to reduce significantly the P-waves (except inside both spherical cones along the vertical line arrangement).

A Specific Magnitude Budget, with the relevant elementary approximations, is relatively enough accurate to compare unambiguously the energy of the stress drop over the fault rupture and the energy of the radiated seismic waves.

Indeed, for the largest natural earthquakes precisely recorded ($6.9 \leq M_w \leq 7.3$), we define very conservatively their average seismic radiation efficiency to 0.25. It follows from that definition, the natural seismic radiation efficiency ranges between 0.113 and 0.520 around the average 0.269 (the natural Specific Magnitude Budget range between $\Delta_{nat}^{min} M_Z = -0.630$ and $\Delta_{nat}^{max} M_Z = -0.189$ around the average $\Delta_{nat}^{mean} M_Z = -0.380$).

On the other hand, the nuclear seismic radiation efficiency ranges between 1.185 and 1.113 around the average 81.9 (the nuclear Specific Magnitude Budget range between $\Delta_{nuc}^{min} M_Z = 0.049$ and $\Delta_{nuc}^{max} M_Z = 2.031$ around the average $\Delta_{nuc}^{mean} M_Z = 1.275$).

In practice, the natural seismic radiation efficiency is always $2.278\times$ times smaller or more than the nuclear seismic radiation efficiency (an artificial gap of the Specific Magnitude Budget $\Delta_{gap} M_Z = 0.238$ is found). Indeed, to provoke a more powerful stress drop over the fault rupture with multiple underground explosions, an accurate information about the future epicenters should be known which is impossible in practice. Lowering too much the energy of the multiple underground nuclear explosions would also increase the risk of not triggering at all the rupture of a seismic fault.

Japan was hit 10 times, United States were hit 4 times, Mexico was hit 4 times, New Zealand was hit 3 times, Italy was hit 2 times. Romania, Ecuador, Peru, Turkey, Croatia, Haiti, Chile, Algeria and Taiwan were hit once time.

The direct costs of the earthquake damages was increased by +390% because of the nuclear earthquakes (1 666 G\$ in total instead of 340 G\$ for the natural earthquakes only). The indirect costs of the more expensive buildings, with respect to the stronger safety standards induced by the 32 giant nuclear earthquakes, are

60 000 G\$ about over the last 40 years.

There is a year anomaly, the nuclear earthquakes does not occurred on a gap of 80.4 days over the 365 days of the year. The probability of that anomaly is 0.57% about. (The nuclear earthquakes occurred only between the day 12.9 and the day 297.3 of the year with UTC).

There is also a day anomaly, 5 nuclear earthquakes have an UTC or a local time so extremely close to midnight. The probability of that anomaly is 0.44% about.

There is also a day anomaly, 5 nuclear earthquakes have an UTC or a local time so extremely close to midnight on the 17th of the month. The probability of that anomaly is 0.51% about.

The Energy Budget may have been used incorrectly in the following article: "Observational constraints on the fracture energy of subduction zone earthquakes" written by Venkataraman, Anupama and Kanamori, Hiroo in 2004 (Figure 16).

Some characteristic infrastructure damages of the 32 giant nuclear earthquakes are illustrated by the Figures 8, 9, 10, 12, 13 and 14.

A list of comments about the historical political contexts of the 32 giant nuclear earthquakes :

- 1- The art of terrorism is tenfold : 1) Doing actions that seem impossible to do with catastrophic & strategic consequences, 2) Passing actions off as accidental and/or from external causes, 3) Appearing incompetent/unprofessional and/or Appearing subject to external constraints and/or Appearing suffering from terrorism, 4) Choosing the critical timing, 5) Choosing the critical location, 6) Keeping action information secret and/or spreading popular/viral/confusing/subtle disinformation, 7) Identity change of the terrorist organization and/or disguise the terrorist organization purge as an accidental/natural disaster, 8) Organizing major/spectacular actions that take a lot of investigations resources with minor consequences. 9) Create global disasters that reduce the investigation intelligence, 10) Terrorism by reproducing/amplifying previous known natural disasters to double down the terror about it and complaining about other irrelevant terrorist attacks.
- 2- The soviet propaganda about the Kola Superdeep Borehole was intended to give the impression that there were completely abnormal, mysterious and unknown phenomena at depths beyond 8 km. The Soviet propaganda was also intended to give the impression it was much more complicate and extremely hard to reach depths beyond 8 km by not reaching at all the official target depth (15 000 meters). The official drilling of the the Kola Superdeep Borehole started 5 years after the first nuclear earthquake in Agadir 1960.

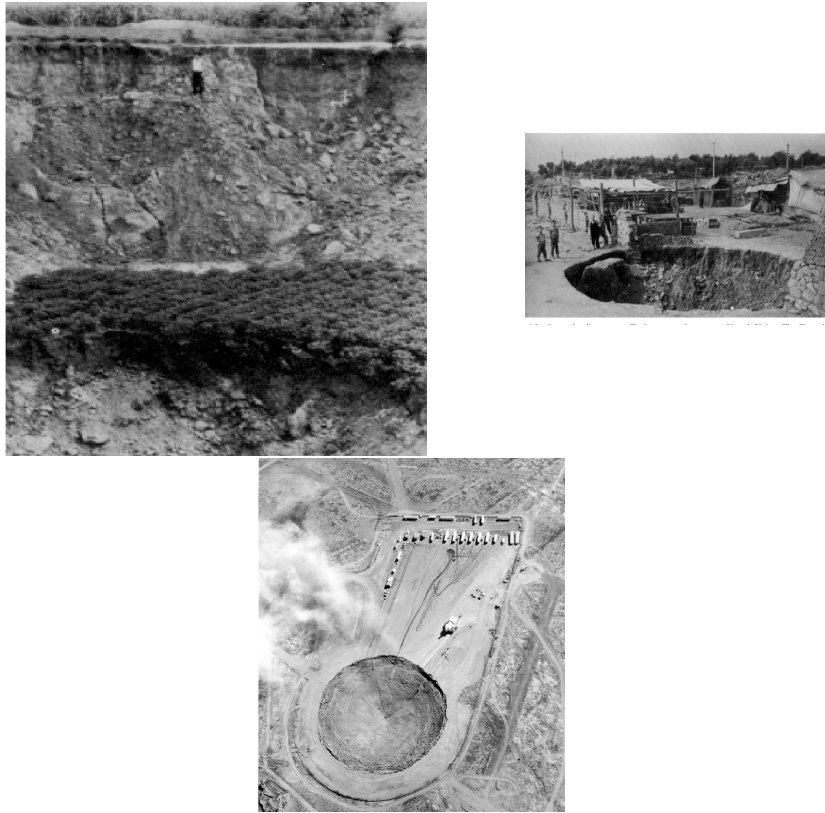


FIGURE 8. Earthquake in Tangshan 1976 and the Nevada test site with underground nuclear tests. The crater in Tangshan 1976 could be a crater from the collapse of a very deep and very large cavity formed by an underground nuclear explosion in Tangshan 1976.

- 3- The first nuclear earthquake on American ground in San Fernando 1971 happened within the Vietnam war context and the Laos war context:

Because of significant logistical stockpiling by PAVN in the Laotian Panhandle, South Vietnam launched Operation Lam Son 719, a military thrust on 8 February 1971. Its goals were to cross into Laos toward the city of Tchepone and cut the Ho Chi Minh Trail, hopefully thwarting a planned North Vietnamese offensive. Aerial support by the U.S. was massive since no American ground units could participate in the operation. On 25 February, PAVN launched a counterattack, and in the face of heavy opposition, the South Vietnamese force withdrew from Laos after losing approximately a third of its men.

The 1971 San Fernando earthquake (also known as the 1971 Sylmar earthquake) occurred in the early morning of February 9 in the foothills of the San Gabriel Mountains in southern California. The event affected a number of health-care facilities in Sylmar, San Fernando, and other densely



FIGURE 9. Characteristic building damages from a suspected nuclear earthquake in Tangshan 1976 and two other nuclear earthquakes in Northridge 1994 and in Hanshin 1995. Relatively light building damages from a natural M_w 7.9 earthquake in San Francisco 1906 at only a hypocentral distance of 15.5 km and triggered by the rupture of the giant San Andreas Fault.

populated areas north of central Los Angeles. The Olive View Medical Center and Veterans Hospital both experienced very heavy damage, and buildings collapsed at both sites, causing the majority of deaths that occurred. The buildings at both facilities were constructed with mixed styles, but engineers were unable to thoroughly study the buildings' responses because they were not outfitted with instruments for recording strong ground motion, and this prompted the Veterans Administration to later install seismometers at its high-risk sites.

- 4- With a 90%-95% confidence level, the earthquake in Tangshan 1976 is also a nuclear earthquake with a Specific Energy Budget between $1.98 \times - 5.69 \times$ (1-sigma interval about) or a Specific Magnitude Budget ΔM_Z between 0.20 - 0.50 (1-sigma interval about).

Like the other 32 giant nuclear earthquakes, there was a large ratio between the vertical ground acceleration and the horizontal acceleration:

Strong motion records obtained on ground during the main shock in Tangshan 1976 show a rather strong vertical component, with max. vertical acceleration about 50%-100% of that of the horizontal even at epicenter

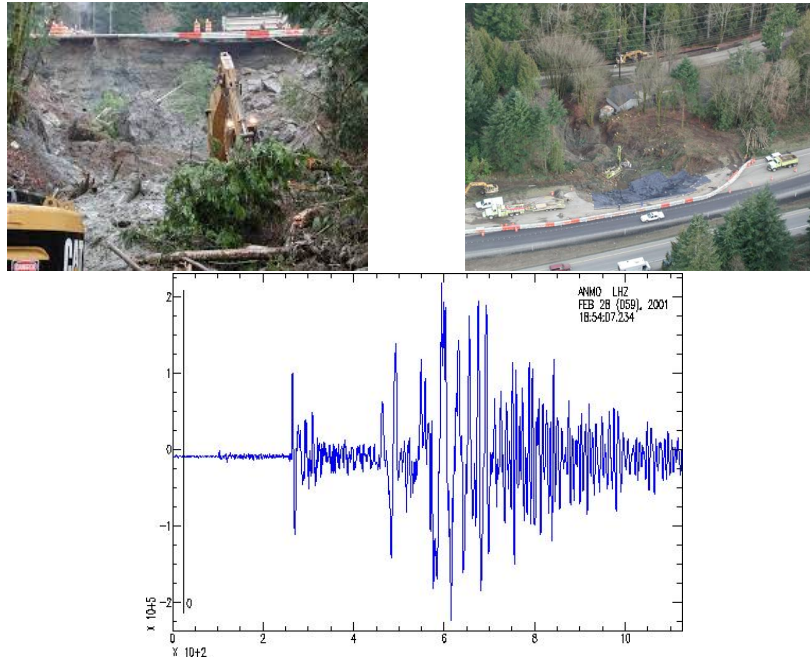


FIGURE 10. It could be a crater from the collapse of a very deep and very large cavity formed by an underground nuclear explosion in Nisqually 2001. The last plot show some initial anomalous strong P-waves of the 2001 Nisqually earthquake at a distance of 1 917 km recorded at the Seismic Station IU ANMO Albuquerque, New Mexico, USA. Since the epicenter was relatively deep (57 km), smaller nuclear pre-explosions (with a small horizontal alignment) may have been done in order to reduce the first P-waves around the epicenter. Then, the S-waves of the smaller nuclear pre-explosions mask the P-waves of the main nuclear explosions (with a vertical line alignment). However, the P-wave of the smaller nuclear pre-explosions are relatively strong far way of the epicenter (horizontal plane) and the seismic attenuation is larger far away for the S-waves than the relatively strong P-waves. Therefore, there is a strong initial peak of the P-waves of the smaller nuclear pre-explosions.

distance more than 100 km, and a long duration nearly 100 seconds at that distance.

Like the other 32 giant nuclear earthquakes, there was that characteristic building damage at the Figure 10 of the page 17 of the article "1976 Tangshan, China Earthquake" written by J .A. Blume (Figure 9).

- 5- Very probably, that giant removal in Human Resources was done for of a giant top secret military program of Nuclear-Powered Subterrenes in Russia : Khrushchev withdrew 1,400 Soviet technicians from the PRC, which

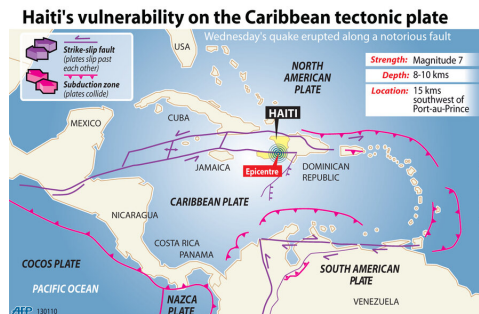


FIGURE 11. Port-au-Prince is located inside a double seismic strike-slip fault system. Therefore, the stress energy accumulated inside that seismic system is released more easily and more frequently BUT at a smaller powerful level. Therefore, it is very unlikely that there will be a natural earthquake as strong as the one that hit Port-au-Prince in 2010.

canceled some 200 joint scientific projects. In response, Mao justified his belief that Khrushchev had somehow caused China's great economic failures and the famines that occurred in the period of the Great Leap Forward.

- 6- April 29 1976 – Sino-Soviet split: A concealed bomb explodes at the gates of the Soviet embassy in China, killing four Chinese. The targets were embassy employees, returning from lunch, but on this day they had returned to the embassy earlier. That event took place exactly 3 months before the suspected nuclear earthquake in Tangshan 1976.
- 7- Romania, already without Soviet troops on its soil, stopped participating in Warsaw Pact troop exercises in 1962. The least active member of the Comecon, Romania was a member of the International Monetary Fund and the World Bank. It owed much of its economic leeway to its oil and grain production, which freed it from Soviet economic leverage.

In March 1964, the Romanian Workers' Party publicly announced the intention of the Bucharest authorities to mediate the Sino-Soviet conflict. In reality, however, the Romanian mediation approach represented only a pretext for forging a Sino-Romanian rapprochement, without arousing the Soviets' suspicions.

In 1974, Romania denied a Soviet request to build a railway from Odessa across eastern Romania to Varna. This broad-gauge railroad could have been used to transport major army units to Bulgaria. Romania opposed the use of its territory by foreign forces, and was the only Warsaw Pact member not to allow the stationing of foreign troops on its soil, Soviet or otherwise. Although Romania did participate in joint Warsaw Pact air and naval exercises, it did not allow such exercises on its own territory. In addition to not allowing Warsaw Pact maneuvers or Soviet bases in Romania,

Ceausescu ended Soviet indoctrination and training in the Romanian Army, and prevented Soviet officers from interfering in decisions of Romanian personnel.

- 8- ONLY 4 days after the USSR made the big Helsinki Accords with the western countries, the worst Dam Failure in human history occurred in Banqiao 1975. Few weeks before the nuclear earthquake in Turkey-Syria 2023: Ankara asked Damascus in Moscow to recognise the YPG as a “terrorist” organisation. Two months before that nuclear earthquake: Turkey has threatened to send group troops into northeastern Syria in retaliation for a deadly Istanbul bombing on November 13 that President Recep Tayyip Erdogan attributes to the Syrian Kurdish YPG (strongly supported by the the Turkish Marxist-Leninist Communist Party). Dugin has killed his own journalist daughter to keep some secrets about Sars-Cov-2 and/or about nuclear earthquakes?
- 9- The 11/09/2001 attacks in New York City occurred EXACTLY 30 years after the death of Nikita Sergeyevich Khrushchev. The Gyrotrons, the giant program of Nuclear-Powered Subterrenes, the Kola Superdeep Borehole, the Soviet space program, the nuclear Kyshtym disaster, the Cuban Missile Crisis and the Sino-Soviet split started under the Khrushchev’s leadership or very soon after it (Figure 15). Napoleon, Mussolini, Khrushchev, Medvedev and Putin may had the Napoleon-complex: little men may try to compensate a lack of physical strength by displaying an extreme drive, ambition, and self-confidence (Figure 15). The Napoleon-complex suggests that shorter men are more likely to have megalomania feelings, initiate conflicts more frequently and respond aggressively to any threat or provocation. Khrushchev was one of the most watched and isolated rulers during his whole retirement. Khrushchev was almost under a regime of semi-liberty during his whole retirement. Probably, that forced and watched isolation during the Khrushchev’s retirement was the consequence of a giant top secret military program of Nuclear-Powered Subterrenes (responsible of the nuclear Kyshtym disaster? The Cuban Missile Crisis was made as a military distraction for USA?).
- 10- The Kaprun disaster was a fire that occurred in an ascending train in the tunnel of the Gletscherbahn Kaprun 2 funicular in Kaprun, Austria, on 11/11/ 2000. The disaster killed 155 people. The inquest ends on September 6, 2001. The 11/09/2001 attacks in New York City. The 04/10/2001, a Soviet S-200 missile shot down a commercial plane above the black sea, most of the passengers were Israelis visiting their relatives in Russia. The Tohoku nuclear earthquake occurred the 11/03/2011.
- 11- 222 days after Russia has Declared Greece “Unfriendly” Country the 22th July 2022, Greece experienced its worst train crash. The worst Greek train crash happened just before the Greek General Elections and the train was completely filled with young graduates. Safety standards were always low

in Greece the last 60 years BUT Greece was never in the sights of a very sophisticated terrorist state until very recently. On the night of 29/10/2022, a crowd crush of young people occurred during Halloween festivities in the Itaewon neighborhood of Seoul, South Korea.

- 13- Earthquake in Tangshan 1976 and the Nevada test site with underground nuclear tests (Figure 8). The crater in Tangshan 1976 could be a crater from the collapse of a very deep and very large cavity formed by an underground nuclear explosion in Tangshan 1976 (Figure 8).
- 13- Characteristic building damages from a suspected nuclear earthquake in Tangshan 1976 and two other nuclear earthquakes in Northridge 1994 and in Hanshin 1995. Relatively light building damages from a natural M_w 7.9 earthquake in San Francisco 1906 at only a hypocentral distance of 15.5 km and triggered by the rupture of the giant San Andreas Fault (Figure 9).
- 14- It could be a crater from the collapse of a very deep and very large cavity formed by an underground nuclear explosion in Nisqually 2001 (Figure 10). The last plot show some initial anomalous strong P-waves of the 2001 Nisqually earthquake at a distance of 1 917 km recorded at the Seismic Station IU ANMO Albuquerque, New Mexico, USA (Figure 10). Since the epicenter was relatively deep (57 km), smaller nuclear pre-explosions (with a small horizontal alignment) may have been done in order to reduce the first P-waves around the epicenter. Then, the S-waves of the smaller nuclear pre-explosions mask the P-waves of the main nuclear explosions (with a vertical line alignment). However, the P-wave of the smaller nuclear pre-explosions are relatively strong far way of the epicenter (horizontal plane) and the seismic attenuation is larger far away for the S-waves than the relatively strong P-waves. Therefore, there is a strong initial peak of the P-waves of the smaller nuclear pre-explosions (Figure 10).
- 15- Port-au-Prince is located inside a double seismic strike-slip fault system. Therefore, the stress energy accumulated in that seismic system is released more easily and more frequently BUT at a smaller powerful level. Therefore, it is very unlikely that there will be a natural earthquake as strong as the one that hit Port-au-Prince in 2010 (Figure 11).

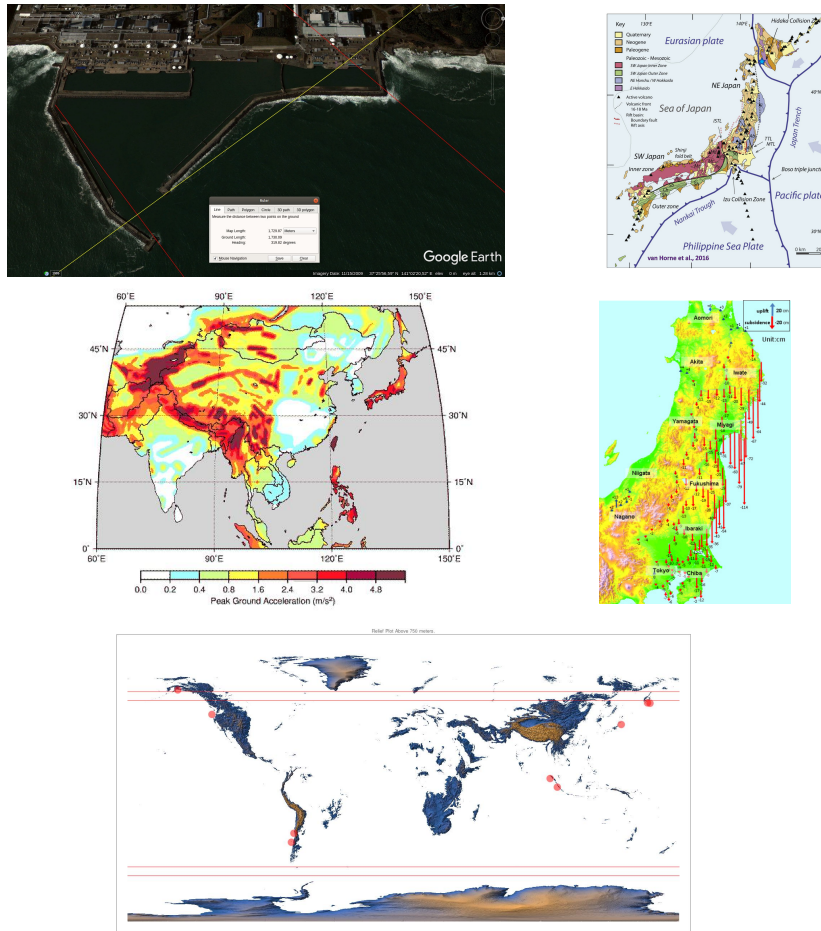


FIGURE 12. The Fukushima Daiichi nuclear disaster was DESIGNED? It was the only nuclear plant with a concave sea wall instead of having a convex sea walls like the Fukushima Daini nuclear plant. The tsunami direction had exactly the right angle (oblique angle of 40° counterclockwise) to lean on the sea wall of the reactors 5 & 6 and being redirected to the reactors 1 & 2 & 3 & 4 at a perpendicular angle with the concave sea wall. Moreover, there is only 0.6% probability to have so many M_w 9.1 earthquakes the last 70 years with respect to the records of the 450 years earlier. Secondly, the other historically known megathrust earthquakes ($M_w \geq 9.1$) only happened near high mountain chains arranged in double lines unlike the 2011 Tōhoku earthquake not near from any high mountains. Thirdly, the fault bends significantly 212 km northwest of the epicenter and makes a complete fault rupture almost impossible as required for a M_w 9.1 earthquake. Finally, the Okhotsk plate subsided instead of uplifting as it would be expected for an Oceanic Subduction Zone.

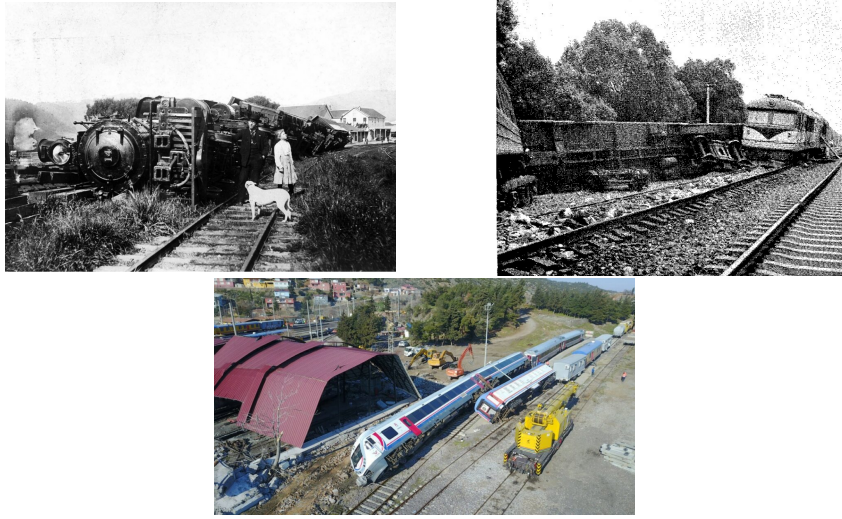


FIGURE 13. The natural earthquake in San Francisco 1906, the nuclear earthquake in Tangshan 1976 and the nuclear earthquake in Turkey–Syria 2023 have overturned few trains. HOWEVER, the train overturned by a natural earthquake in San Francisco 1906 was ON the giant San Andreas Fault at Point Reyes, United States.

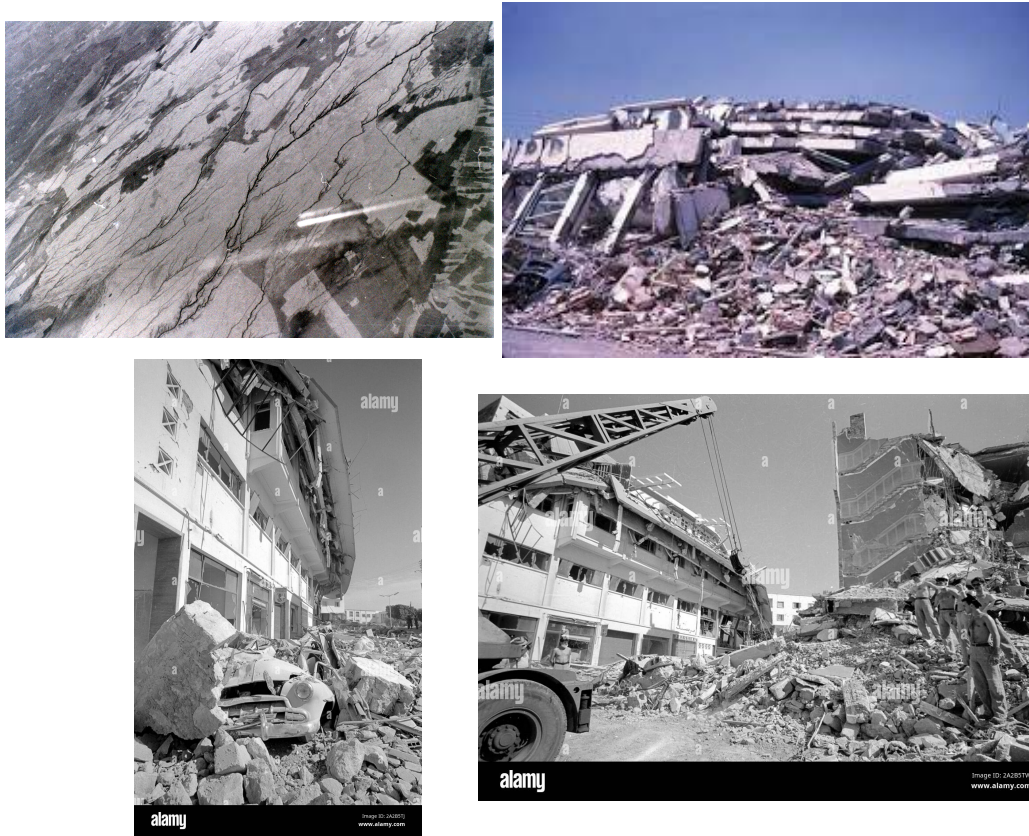


FIGURE 14. Characteristic building damages from a suspected nuclear earthquake in Agadir 1960 with an existing very low natural seismic hazard and risk. Multiple thin cracks on a flat ground with a large dispersion.



FIGURE 15. Characteristic building damages from a suspected nuclear earthquake in Agadir 1960 with an existing very low natural seismic hazard and risk. Multiple thin cracks on a flat ground with a large dispersion.



FIGURE 16. Characteristic building damages from a suspected nuclear earthquake in Skopje 1963.



FIGURE 17. The direct influence of Nikita Khrushchev over Josip Tito one month after the Russian nuclear earthquake in Skopje 1963.



FIGURE 18. Earthquake Montenegro 1979, Shape of the coastal landscape with its dry valleys and other spectacular features from a large natural seismic normal fault with a privileged direction.



FIGURE 19. The 2023 Turkey-Syria earthquake created a canyon 35 meters deep and 200 meters wide. It could be a land subsidence from the collapse of a very deep and very large cavity formed by an underground nuclear explosion.

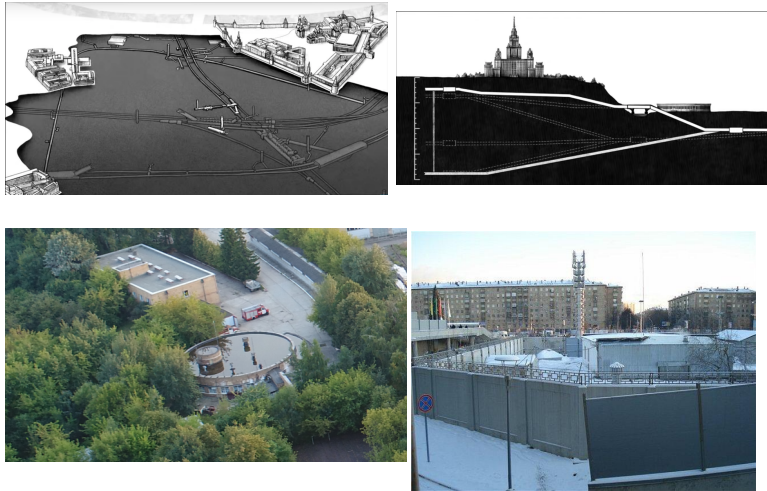


FIGURE 20. Secret and Anomalous underground activities in Russia : Moscow Metro-2. A surface building of Matveevsky air intake (DV-1) with ventilation shafts



FIGURE 21. Secret and Anomalous underground activities in Russia : Moscow Metro-2. A hermetic gate in a deep single track tunnel that separates Metro-1 from Metro-2, which was built after transferring this tunnel to KGB



FIGURE 22. Secret and Anomalous underground activities in Russia : the fast expanding giant Batagaika crater.



FIGURE 23. Secret and Anomalous underground activities in Russia : Various mysterious craters in the Yamal peninsula.

16- The Fukushima Daiichi nuclear disaster was DESIGNED? It was the only nuclear plant with a concave sea wall instead of having a convex sea walls like the Fukushima Daini nuclear plant. The tsunami direction had exactly the right angle (oblique angle of 40° counterclockwise) to lean on the sea wall of the reactors 5 & 6 and being redirected to the reactors 1 & 2 & 3 & 4 at a perpendicular angle with the concave sea wall (Figure 12). Moreover, there is only 0.6% probability to have so many M_w 9.1 earthquakes the last 70 years with respect to the records of the 450 years earlier. Secondly, the other historically known megathrust earthquakes ($M_w \geq 9.1$) only happened near high mountain chains arranged in double lines unlike the 2011 Tōhoku earthquake not near from any high mountains (Figure 12). Thirdly, the fault bends significantly 212 km northwest of the epicenter and makes a complete fault rupture almost impossible as required for a M_w 9.1 earthquake (Figure 12). Finally, the Okhotsk plate subsided instead of up-lifting as it would be expected for an Oceanic Subduction Zone (Figure 12).

There is no mountains above 2 000 meters in the double latitude gap delimited by the horizontal red lines because the ice erosion is maximal (Figure 12). We do not consider the observed inundation at the Makauwahi sinkhole on Kaua'i as a proof for a megathrust earthquake ($M_w \geq 9.25$) in Aleutian Islands 1585 which would be the presumed source of a tsunami along the Sanriku coast of Japan on June 11, 1585, known only from vague historical accounts and oral traditions. Indeed, that event was initially misdated to 1586 and a megathrust earthquake in Cascadia would create a tsunami with a better orientation for the Makauwahi sinkhole on Kaua'i and for the Sanriku coast of Japan.

17- The weight of the multiple nuclear H-bombs in Tohoku 2011 is roughly the weight of $8\times$ times the Statue of Liberty or $3\times$ times the Payload to LEO of the Sea Dragon Rocket:

$$\begin{aligned}
 r_H &\cong (17.59)/(6.015122 + 2.014101)/931.49 \times 9\,000 \times 10^{16} \\
 (24) \quad &\cong 2.117 \times 10^{17} \text{ J/ton} \\
 M_H &\cong 1/C_Z \times E_{7.0} \times 31.61^{0.897(M_w-7.0)} R_Z / (41.95\% \times r_H) \\
 &\cong 18.414 \times 1\,995 \times 10^{12} \times 31.61^{0.8978 \times (9.1-7.0)} \times 5.926 / (0.4195 \times 2.117 \times 10^{17}) \\
 (25) \quad &\cong 1\,650 \text{ tons}
 \end{aligned}$$

The weight of the multiple nuclear H-bombs in Chiapas 2017 is roughly the weight of $36\times$ times the Statue of Liberty or $13\times$ times the Payload to LEO of the Sea Dragon Rocket:

$$\begin{aligned}
 M_H &\cong 1/C_Z \times E_{7.0} \times 31.61^{0.897(M_w-7.0)} R_Z / (41.95\% \times r_H) \\
 &\cong 18.414 \times 1\,995 \times 10^{12} \times 31.61^{0.8978 \times (8.1-7.0)} \times 587.7 / (0.4195 \times 2.117 \times 10^{17}) \\
 (26) \quad &\cong 7\,365 \text{ tons}
 \end{aligned}$$

- 18- The nuclear earthquake in Haiti 2010 and the nuclear earthquake in Turkey-Syria 2023 may have been chosen to occur during the electoral campaign of the general elections and during a period of heavy rains. That critical timing is chosen in order to increase the nuclear earthquake devastation with the soil liquefaction and to make more difficult the rescue operations at a critical political time. The Haiti place may have been chosen to circumvent the United States embargo against Cuba by destabilizing neighboring countries (Cubans travel to Haiti searching for shopping bargains) and the Turkey-Syria place may have been chosen to reduce the number of Russian soldiers needed in Syria during the Ukraine war launched by Russia.
- 19- The natural earthquake in San Francisco 1906, the nuclear earthquake in Tangshan 1976 and the nuclear earthquake in Turkey-Syria 2023 have overturned few trains. HOWEVER, the train overturned by a natural earthquake in 1906 was ON the giant San Andreas Fault (Figure 13).
- 20- The 2023 Turkey-Syria earthquake created a canyon 35 meters deep and 200 meters wide. It could be a land subsidence from the collapse of a very deep and very large cavity formed by an underground nuclear explosion (Figure 14).
- 21- The Russian international terrorism globally pushes to increase the use of contactless technologies, to increase the digitalization of human activities, to increase the urban sprawl, to increase the redundancy of safety standards and to raise the level of safety standards.
- 22- Within the context of the 36 giant nuclear earthquakes, the Chernobyl accident was fake and used for two purposes. The first one is to show a fake easily detectable unprofessional appearance with respect to the nuclear energy. The second one is to ensure a secrecy at an extremely high level within the Russian Federation by doing a PLANNED purge of political dissidents by sending them to deadly radioactive areas for unsafe decontamination work or by delaying their evacuations or giving them permanent jobs years ago in the Chernobyl region. The Russian Federation may have used some dirty nuclear activities as a "Final Solution" against political dissidents.
- 23- The Russian Federation may have created the LONG COVID disease as an attempt to globally reduce the intelligence of investigations about the 36 giant nuclear earthquakes around the world that have struck large urban areas subject to an existing Natural Seismic Hazard (nuclear explosions are spatially arranged and temporally synchronized to reduce the P-waves and to trigger the rupture of the existing seismic faults).
- 24- A Natural Seismic Hazard is an unwanted indirect consequence of the large reduction of the cosmic rays on the Earth's surface. A strong Earth's magnetic field is needed to avoid the Earth's atmosphere erosion from the solar flares. A strong Earth's magnetic field is possible only with a powerful Dynamo Mechanism creating also an unwanted Natural Seismic Hazard.

The Nuclear Technologies has reduced the natural benefits of the powerful Earth's Dynamo Mechanism by amplifying significantly and subtly the existing Natural Seismic Hazard with 36 giant nuclear earthquakes. Finally, the Symmetric Deterrence theory does not hold at all to avoid an irreversible nuclear escalation but rather an Extreme Asymmetric Development holds to avoid a nuclear escalation. In the last case, both sides try to "win" in a very different way and in a very difficult way without a central point of contact between both sides. Within a Symmetric Deterrence theory, there is always a central point of contact between both sides which creates an exponential escalation reaching relatively fast the irreversible nuclear escalation level. In the current Extreme Asymmetric Development, one side tries to "win" by compromising significantly the economic development of the other side with a massive use of the nuclear technology in a hidden way and in an inefficient way and without any detectable nuclear fallout (an inefficient way using an extremely compact source of energy is still a very strong way as it is the case for the 36 giant nuclear earthquakes). The second side tries to "win" by increasing massively its own economic development with stronger and stronger safety standards and by exploiting more and more its natural resources. Both sides can not exclude they have a "winnable" strategy in that Extreme Asymmetric Development and there is no central point of contact between both sides that could trigger an exponential escalation. Finally, the fact that the nuclear technology was ONLY used within 4 days and within 300 km to kill directly & massively other humans over the last 78 years worldwide is just a MYTH (Atomic bombings of Hiroshima and Nagasaki).

- 25- Perhaps, the next step in trying to make nuclear earthquakes forget is to detonate a few small nuclear bombs in Ukraine. It may be a sketch already carefully decided in advance, the Russian army loses "too much" and is "forced" to use a few small tactical nuclear bombs in its "forced retirement" from Ukraine. Everyone is obsessed with those potential events and no one is thinking at all about giant nuclear earthquakes.... who knows?
- 26- The earthquake Agadir 1960 has been the very first nuclear Russian earthquake in an area with a very low seismic hazard. Moreover, it has happened just few minutes before the 1st March like the Tempa train crash in Greece 2023. It has also happened just 2 weeks after the very first French atomic test in Sahara. Finally, Morocco was a very strategic place during the Cold War since that country is bordering both the Atlantic and the Mediterranean coast. The only logical explanation for this so early Russian nuclear earthquake in Agadir in 1960 is to consider Adolf Hitler's secret surrender to the Soviet Union taking with him the vast majority of Nazi Germany's nuclear/technological/military secrets shortly before the end of World War II.



FIGURE 24. Nikita Sergeyevich Khrushchev had the Napoleon-complex? It is very logical the USSR had a giant top secret military program of Nuclear-Powered Subterrenes to make many giant nuclear earthquakes since they were strongly opposed against the capitalism property in a general way.

Did Khrushchev poison Marilyn Monroe on 09/19/1959 in order to make a martyr of the most famous communist sympathizer in the United States?

Khrushchev inspected her closely as he shook her hand. "You're a very lovely young lady," he said.

Back home, Marilyn told her maid what she really thought of Khrushchev. He was fat and ugly and had warts on his face and he growled," she said. "He squeezed my hand so long and hard that I thought he would break it. I guess it was better than having to kiss him.

For a deep event, the energy radiated in the P - and S -waves can be estimated directly from measurements of the energy flux in the body-wave arrivals. Neglecting directivity, *Boatwright and Fletcher* [1984] derived the "point source" formulae

$$E_s^P = 4\pi \langle F^P \rangle^2 \left(\frac{R^3}{F^3} \right) \epsilon_{sP}^* \quad (1a)$$

$$E_s^S = 4\pi \langle F^S \rangle^2 \left(\frac{R^3}{F^3} \right) \epsilon_{sS}^* \quad (1b)$$

relating the total energy radiated in the body wave (E_s^P or E_s^S) to the energy flux contained in the P - or S -wave arrival.

radiation patterns. The seismic moment is then given by the relation,

$$M_0 = 4\pi \rho a^3 \frac{R}{F^3} \bar{u} \quad (28)$$

The results of this analysis are compiled in Table 3; the average estimate of the seismic moment is $M_0 = (1.7 \pm 0.3) \times 10^{26}$ dyn cm, similar to the estimate of 1.7×10^{26} dyn cm estimated from the long-period GDSN data by S. A. Sipkin (personal communication, 1984) and $(1.85 \pm 0.16) \times 10^{26}$ dyn cm estimated from the long-period WSSN body waves by *Barrientos et al.* [1985]. *Doser and Smith* [1985] estimated the moment as $1.6\text{--}2.1 \times 10^{26}$ dyn cm from a moment inversion of long period SRO data. We note that this is a long-period estimate, rather than a broad-band estimate, although the corner period of the Borah Peak earthquake (≈ 13 s) is nearer to the 20-s period range than that of the Coalinga earthquake. Combining this moment with the radiated energy estimate corrected for the horizontal focussing of energy gives $\tau_c = 6.8 \pm 1.3$ bars.

MEASUREMENT OF THE ENERGY FLUX
 As discussed by *Boatwright et al.* [1983] and *Boatwright and Fletcher* [1984] for near-field data, the noise and the attenuation characteristics critically affect the correction of the "radiated" energy flux. In this section, we consider how these factors can be corrected for. The correction for the attenuation of the energy flux in a plane wave can be calculated from the position of the detector, the wave velocity, and the integral of the square of the ground velocity.

$v_s = \int_{v_s} v_s^2 dt = \rho \int_{v_s} v_s^2 dt$ (16)

where the integration extends over the duration of the body-wave arrival. To correct the measurement for the attenuation, the power spectrum of the ground velocity can be used to replace the integral in equation (16) with an integral over angular frequency. The correction for the attenuation is determined using the function $\langle v_s^2 \rangle = \langle v_s^2 \rangle$ in the integral over angular frequency.

$v_s^2 = \frac{1}{\rho} \int_{v_s} \rho v_s^2 dt = \rho \int_{v_s} v_s^2 dt$ (17)

For this analysis, we will use the description of v_s^2 determined by *Lee et al.* [1981, 1982, unpublished observations]. Their results are plotted in Figure 6, along with the approximation:

$v_s^2 = 0.8 - 0.3 \ln v_s / f < 1 \text{ Hz}$
 $v_s^2 = 0.8 - 0.7 \ln v_s / f > 1 \text{ Hz}$ (18)

used to correct the energy flux measurements for the attenuation defined on the Richter's U.S. Shook paths.

In transforming from equation (16) to equation (17), the square of the time-average of the ground velocity is replaced by the power spectrum of the ground velocity. The range of integration in equation (17) extends to infinite frequency. Unfortunately, the power spectrum of the ground velocity can be reliably determined only for a limited frequency band. Figure 7 shows a comparison of the measured spectrum with a function of frequency for three of the gP waveforms radiated by the Borah Peak earthquake and the gS waveforms radiated by the Coalinga earthquake. The mean amplitudes are taken from the data shown in Figures 2 and 4 and the gS waveforms just before the body-wave arrival. The gP spots at stations

and 2001 (shown on the location map in Figure 2), we used P wave teleseismic data recorded at broadband stations around the world and archived at the IRIS Data Management Center. Only the vertical component data (BHZ channel) of stations at distances between 30° and 90° were used in this study. We applied corrections for path and radiation pattern [*Boatwright and Choy*, 1988], to determine the moment rate spectrum ($\dot{M}(f)$) from the displacement spectrum ($\hat{u}(f)$) at a station using

$$\dot{M}(f) = \frac{4\pi \rho v_s^3 R_0^2 \sin^2 \theta |u(f)|}{g(\lambda) R(\theta, \phi) C |r(f)|}$$

where θ is the teleseismic distance, the geometric spreading factor $1/r$ is replaced by $g(\lambda)/R_0$, $R_0 = 6371$ km is the radius of the earth, v_s is the P wave or S wave velocity, r is the attenuation factor (equal to the travel time divided by the path-averaged Q factor), C is the free surface receiver effect, and $r(f)$ is the instrument response. By integrating the squared moment rate spectrum determined at each station we computed radiated energy, E_s . Thus

$$E_s = \frac{8\pi}{15\rho v_s^3} \int_{f_1}^{f_2} \dot{M}(f)^2 df$$

where ρ is the density, and α and β are the P and S wave velocities of the medium. We refer to this method of estimating radiated energy as the single-station method. The first and second terms in the parenthesis on the right-hand side of the equation represent contributions from P and S waves, respectively; the P wave contribution is about 5 percent of the S wave contribution. The mean value of

FIGURE 25. The Energy Budget may have been used incorrectly in the following article: "Observational constraints on the fracture energy of subduction zone earthquakes" written by Venkataraman, Anupama and Kanamori, Hiroo in 2004.

Location	Country	Date with UTC	Date with Local time	Days	Hypocentral Depth (km)	M_0	$M_0/0.8978$	$M_0 - M_{0,work}$	E_s/E_{work}	Costs (G\$)
Agadir 1960	Morocco	(1960, 2, 29)	(1960, 2, 29)	0	10	5.8	7.13463	1.19824	62.7057	1.236
Makarska 1962	Yugoslavia	(1962, 1, 11)	(1962, 1, 11)	681.226	15	6.2	7.22083	0.916583	23.6984	0.412
Skojpe 1963	Yugoslavia	(1963, 7, 26)	(1963, 7, 26)	1242.19	6	6.1	7.01428	0.829844	17.9388	11.25
San Fernando 1971	United States	(1971, 2, 9)	(1971, 2, 9)	3997.6	8.4	6.6	6.89454	0.264438	2.49257	1
Vrancea 1977	Romania	(1977, 3, 4)	(1977, 3, 4)	6212.82	85.3	7.5	8.06398	0.586341	5.74767	2.048
Mexico 1985	Mexico	(1985, 9, 19)	(1985, 9, 19)	9333.57	23	8	9.08898	0.986663	30.1965	5
Vrancea 1986	Romania	(1986, 8, 30)	(1986, 8, 30)	9678.91	131	7.3	8.87663	1.4155	132.799	3
Whittier Narrows 1987	United States	(1987, 10, 1)	(1987, 10, 1)	10075.6	14	5.9	6.19759	0.267179	2.51628	0.4
Loma Prieta 1989	Mexico	(1989, 10, 18)	(1989, 10, 17)	10823	19	6.9	7.26816	0.338537	3.13179	6
Kushiro 1993	Japan	(1993, 1, 15)	(1993, 1, 15)	12808.5	108	7.6	8.02276	0.379553	3.70949	0.75
North Ridge 1994	United States	(1994, 1, 17)	(1994, 1, 17)	12375.5	18.2	6.7	7.62486	0.330338	17.5985	59
Great Hanshin 1995	Japan	(1995, 1, 16)	(1995, 1, 17)	12739.9	17.6	6.9	7.37296	0.423819	4.32227	200
Jiji 1999	Taiwan	(1999, 8, 17)	(1999, 8, 17)	14413	12	7.65	8.12243	0.424152	4.32725	10
Nisqually 2001	United States	(2001, 2, 28)	(2001, 2, 28)	14974.8	57	6.8	7.22914	0.385281	3.78361	2
Geyse 2001	Japan	(2001, 3, 24)	(2001, 3, 24)	14998.3	50	6.9	8.11542	1.09211	43.4627	0.05
Southern Peru 2001	Peru	(2001, 6, 23)	(2001, 6, 23)	15089.9	32	8.4	9.43171	0.92627	24.5115	0.75
Boumerdes 2003	Algeria	(2003, 5, 21)	(2003, 5, 21)	15786.8	12	6.8	7.22486	0.381443	3.73379	5
Chuetsu 2004	Japan	(2004, 10, 23)	(2004, 10, 23)	16307.4	13	6.8	7.75001	0.852919	10.0259	28
Chuetsu 2007	Japan	(2007, 7, 16)	(2007, 7, 16)	17303.1	10	6.6	6.65477	0.0491761	1.18512	12.5
Haiti 2010	Haiti	(2010, 1, 12)	(2010, 1, 12)	18214.9	13	7	7.32044	0.287688	2.78098	8.5
Chile 2010	Chile	(2010, 2, 27)	(2010, 2, 27)	18260.3	35	8.8	9.64048	0.754583	13.5471	30
Baja California 2010	Mexico	(2010, 4, 4)	(2010, 4, 4)	18297	10	7.2	7.44851	0.223108	2.16099	1.1
Canterbury 2010	New Zealand	(2010, 9, 3)	(2010, 9, 4)	18448.7	10	7.1	7.24708	0.132052	1.57788	40
Christchurch 2011	New Zealand	(2011, 2, 21)	(2011, 2, 22)	18620	5	6.15	6.47191	0.289011	2.71235	40
Tohoku 2011	Japan	(2011, 3, 11)	(2011, 3, 11)	18637.3	29	9.1	9.67384	0.515196	5.92617	720
Christchurch June 2011	New Zealand	(2011, 6, 13)	(2011, 6, 13)	18731.1	7	6	6.54537	0.489632	5.42537	3
Northern Italy 2012	Italy	(2012, 5, 20)	(2012, 5, 20)	19073.1	14.8	6.1	6.32801	0.204707	2.02793	15.8
Ecuador 2016	Ecuador	(2016, 4, 16)	(2016, 4, 16)	20501	20.6	7.8	7.98448	0.16563	1.7719	3
Central Italy August 2016	Italy	(2016, 8, 24)	(2016, 8, 24)	20630.1	19.2	6.1	7.01493	0.821421	17.0648	5
Chiappas 2017	Mexico	(2017, 9, 8)	(2017, 9, 7)	21010.2	47.4	8.1	10.1563	1.84613	587.66	4
Osaka 2018	Japan	(2018, 6, 17)	(2018, 6, 18)	21293	13	5.6	6.74201	1.02529	34.5066	7
Hokkaido Eastern Ibari 2018	Japan	(2018, 9, 5)	(2018, 9, 6)	21372.8	35	6.6	7.98137	1.24019	72.4837	2
Zagreb 2019	Croatia	(2019, 3, 22)	(2019, 3, 22)	21936.2	10	5.3	5.60676	0.275405	2.58879	11.7
Fukushima 2021	Japan	(2021, 2, 13)	(2021, 2, 13)	22264.6	44	7.1	9.1481	1.83879	572.945	7.7
Fukushima 2022	Japan	(2022, 3, 16)	(2022, 3, 16)	22660.6	41	7.3	9.56225	2.03105	1113	4
Turkey-Syria 2023	Turkey	(2023, 2, 6)	(2023, 2, 6)	22987.1	17.9	7.75	8.55683	0.724372	12.2048	100

FIGURE 26. Raw data of the 36 giant nuclear earthquakes.

Location	Country	Date with UTC	Date with local time	Days	Hypocentral Depth (km)	M_w	$M_0/0.8978$	$M_0 - M_{0crk}$	E_0/E_{0crk}	Costs (G\$)
Valdivia 1960	Chile	(1960, 5, 22)	(1960, 5, 22)	-3914.78	33	9.5	9.24748	-0.226714	0.457022	8
Irpinta 1980	Italy	(1980, 11, 23)	(1980, 11, 23)	3575.19	10	6.9	6.52021	-0.340971	0.308804	15
Coalinga 1983	United States	(1983, 5, 2)	(1983, 5, 2)	4465.4	10	6.7	6.33954	-0.323619	0.327027	0.02
Borah Peak 1983	United States	(1983, 10, 28)	(1983, 10, 28)	4644.	16	6.9	6.31343	-0.526522	0.162213	0.02
Landers 1992	United States	(1992, 6, 28)	(1992, 6, 28)	7809.91	1.09	7.3	7.08926	-0.189201	0.520242	0.1
Izmit 1999	Turkey	(1999, 9, 20)	(1999, 9, 21)	10450.2	15	7.6	7.15766	-0.397136	0.253695	20
Aquila 2009	Italy	(2009, 4, 6)	(2009, 4, 6)	13935.5	9.46	6.9	6.49636	-0.362384	0.286948	16
Kaohsiung 2010	Taiwan	(2010, 3, 4)	(2010, 3, 4)	14267.4	5	6.3	5.70447	-0.534667	0.157768	1
Kumamoto 2016	Japan	(2016, 4, 15)	(2016, 4, 16)	16502.1	10	7.	6.54575	-0.407825	0.244499	20
Puebla 2017	Mexico	(2017, 9, 19)	(2017, 9, 19)	17024.2	54.5	7.2	6.73397	-0.4184	0.23573	8
Ridgecrest 2019	United States	(2019, 7, 6)	(2019, 7, 5)	17678.6	8	7.1	6.50077	-0.537986	0.15597	5.3
Albania 2019	Albania	(2019, 11, 26)	(2019, 11, 26)	17821.5	20	6.6	6.08098	-0.465976	0.209011	1
Petrinja 2019	Croatia	(2020, 12, 29)	(2020, 12, 29)	18220.9	4.4	6.4	6.09446	-0.274318	0.387734	5
Haiti 2021	Haiti	(2021, 8, 14)	(2021, 8, 14)	18448.9	10	7.2	6.71725	-0.433415	0.223817	1.5
Tai tung 2022	Taiwan	(2022, 9, 18)	(2022, 9, 18)	18448.7	7.3	6.9	6.1982	-0.638078	0.113477	0.147

FIGURE 27. Raw data of some 16 natural earthquakes.

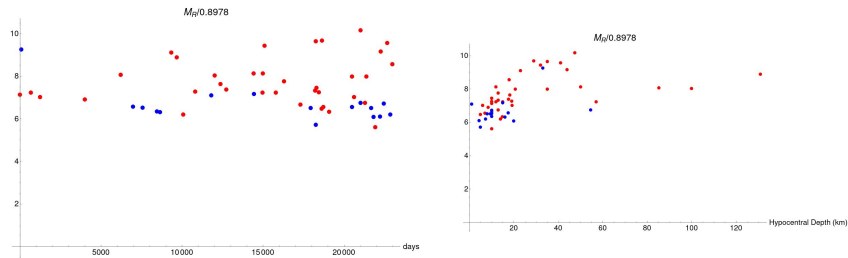


FIGURE 28. The abscissa of the first plot is the number of days of the earthquakes from the first nuclear earthquake in Agadir 1960. The ordinate is the radiated magnitude normalized as the moment magnitude (they are equal if the energy of the radiated seismic waves is equal to the energy of the stress drop over the fault rupture).

REFERENCES

- [1] A. Zaganidis, “Mathematica Notebooks, Pictures and Source Files: A specific magnitude budget for the detection of 30 nuclear earthquakes in urban areas subject to an existing natural seismic hazard.” https://drive.google.com/drive/folders/1Rid5ZDhbUKgQt1XHSDVGLiYODgAv50AU?usp=share_link.
- [2] R. C. Stewart and P. D. Marshall, “Seismic P-waves from Novaya Zemlya explosions: seeing double!,” *Geophysical Journal International*, vol. 92, pp. 335–338, 02 1988.
- [3] J. Boatwright and G. Choy, “Teleseismic estimates of the energy radiated by shallow earthquakes (usa).,” *Journal of Geophysical Research*, vol. 91, pp. 2095–2112, 02 1986.
- [4] G. Choy and J. Boatwright, “Global patterns of radiated seismic energy and apparent stress,” *Journal of Geophysical Research*, vol. 1001, pp. 18205–18228, 09 1995.
- [5] H. Kanamori, “Chapter 11 energy budget of earthquakes and seismic efficiency,” *International Geophysics*, vol. 76, pp. 293–305, 12 2001.
- [6] A. Venkataraman and H. Kanamori, “Observational constraints on the fracture energy of subduction zone earthquakes,” *Journal of Geophysical Research: Solid Earth*, vol. 109, no. B5, 2004.
- [7] J. Aubry, F. X. Passelègue, D. Deldicque, F. Girault, S. Marty, A. Lahfid, H. S. Bhat, J. Escartin, and A. Schubnel, “Frictional heating processes and energy budget during laboratory earthquakes,” *Geophysical Research Letters*, vol. 45, no. 22, pp. 12,274–12,282, 2018.
- [8] L. Serva, A. Blumetti, L. Guerrieri, and A. Michetti, “The apennine intermountain basins: The result of repeated strong earthquakes over a geological time interval,” vol. 1, pp. 939–946, 01 2002.
- [9] C. Perrin, F. Waldhauser, and C. Scholz, “The shear deformation zone and the smoothing of faults with displacement,” *Journal of Geophysical Research Solid Earth*, vol. 126, pp. 1–18, 05 2021.
- [10] S. Veeraraghavan, T. H. Heaton, and S. Krishnan, “Lower Bounds on Ground Motion at Point Reyes during the 1906 San Francisco Earthquake from Train Toppling Analysis,” *Seismological Research Letters*, vol. 90, pp. 683–691, 01 2019.
- [11] J. A. B. ume, “1976 tangshan, china earthquake (papers presented at the 2nd u.s. national conference on earthquake engineering held at stanford university).” <https://nehrpsearch.nist.gov/static/files/NSF/PB82123175.pdf>, August 22-24, 1979.
- [12] L. Huixian, G. W. Housner, X. Lili, and H. Duxin, “The great tangshan earthquake of 1976,” 2002.
- [13] T. Imakiire and M. Koarai, “Wide-area land subsidence caused by “the 2011 off the pacific coast of tohoku earthquake”,” *Soils and Foundations*, vol. 52, no. 5, pp. 842–855, 2012. Special Issue on Geotechnical Aspects of the 2011 off the Pacific Coast of Tohoku Earthquake.
- [14] M. Matsubara, H. Sato, T. Ishiyama, and A. Van Horne, “Configuration of the moho discontinuity beneath the japanese islands derived from three-dimensional seismic tomography,” *Tectonophysics*, vol. 710-711, pp. 97–107, 2017. Evolution of fore-arc and back-arc sedimentary basins with focus on the Japan subduction system and its analogues.
- [15] J. Patton, “Violent shaking triggers massive landslides in sapporo japan earthquake.” https://static.tumblr.net/wp-content/uploads/2018/09/M66_figure_02_geology_plate_boundaries_blue_star-910x1024.jpg, September 6, 2018.
- [16] R. Butler, D. Burney, and D. Walsh, “Paleotsunami evidence on kuaʻi and numerical modeling of a great aleutian tsunami,” *Geophysical Research Letters*, vol. 41, no. 19, pp. 6795–6802, 2014.
- [17] T. G. S. H. A. P. (GSHAP). <https://www.un-spider.org/links-and-resources/data-sources/global-seismic-hazard-assessment-gshap-icsu>.
- [18] E. F. Plinski, “Gorky’s gyrotron heroes,” 01 2020.
- [19] Wikipedia. https://en.wikipedia.org/wiki/Seismic_magnitude_scales.
- [20] Wikipedia. https://en.wikipedia.org/wiki/Shear_modulus.
- [21] Wikipedia. https://wiki.seg.org/wiki/Seismic_attenuation.
- [22] Wikipedia. https://en.wikipedia.org/wiki/List_of_costliest_earthquakes.
- [23] Wikipedia. https://en.wikipedia.org/wiki/List_of_megathrust_earthquakes.
- [24] Wikipedia. https://en.wikipedia.org/wiki/1906_San_Francisco_earthquake.
- [25] Wikipedia. https://en.wikipedia.org/wiki/Nikita_Khrushchev.

- [26] Wikipedia. https://en.wikipedia.org/wiki/State_visit_by_Nikita_Khrushchev_to_the_United_States.
- [27] Wikipedia. https://en.wikipedia.org/wiki/Sino-Soviet_split.
- [28] Wikipedia. https://en.wikipedia.org/wiki/De-satellization_of_the_Socialist_Republic_of_Romania.
- [29] Wikipedia. <https://en.wikipedia.org/wiki/Gyrotron>.
- [30] Wikipedia. <https://en.wikipedia.org/wiki/Quaise>.
- [31] Wikipedia. <https://en.wikipedia.org/wiki/Subterrene>.
- [32] Wikipedia. [https://en.wikipedia.org/wiki/Gerboise_Bleue_\(nuclear_test\)](https://en.wikipedia.org/wiki/Gerboise_Bleue_(nuclear_test)).
- [33] Wikipedia. https://en.wikipedia.org/wiki/1960_Agadir_earthquake.
- [34] FPIF. https://fpif.org/morocco_and_western_sahara.
- [35] Wikipedia. https://en.wikipedia.org/wiki/1962_Makarska_earthquakes.
- [36] Wikipedia. https://en.wikipedia.org/wiki/1963_Skopje_earthquake.
- [37] Wikipedia. https://en.wikipedia.org/wiki/Cuban_Missile_Crisis.
- [38] Wikipedia. https://en.wikipedia.org/wiki/Kola_Superdeep_Borehole.
- [39] Wikipedia. https://en.wikipedia.org/wiki/Helsinki_Accords.
- [40] Wikipedia. https://en.wikipedia.org/wiki/1975_Banqiao_Dam_failure.
- [41] Wikipedia. https://en.wikipedia.org/wiki/1976_Tangshan_earthquake.
- [42] Wikipedia. https://en.wikipedia.org/wiki/1979_Montenegro_earthquake.
- [43] Wikipedia. https://en.wikipedia.org/wiki/1983_Coalinga_earthquake.
- [44] Wikipedia. https://en.wikipedia.org/wiki/1983_Borah_Peak_earthquake.
- [45] Wikipedia. https://en.wikipedia.org/wiki/1985_Mexico_City_earthquake.
- [46] Wikipedia. https://en.wikipedia.org/wiki/1987_Whittier_Narrows_earthquake.
- [47] Wikipedia. https://en.wikipedia.org/wiki/1992_Landers_earthquake.
- [48] Wikipedia. https://en.wikipedia.org/wiki/1993_Kushiro_earthquake.
- [49] Wikipedia. https://en.wikipedia.org/wiki/1994_Northridge_earthquake.
- [50] Wikipedia. https://en.wikipedia.org/wiki/Great_Hanshin_earthquake.
- [51] Wikipedia. https://en.wikipedia.org/wiki/2001_Nisqually_earthquake.
- [52] Wikipedia. https://en.wikipedia.org/wiki/2001_Geiyo_earthquake.
- [53] Wikipedia. https://en.wikipedia.org/wiki/2001_southern_Peru_earthquake.
- [54] Wikipedia. https://en.wikipedia.org/wiki/2010_Haiti_earthquake.
- [55] Wikipedia. https://en.wikipedia.org/wiki/2010_Kaohsiung_earthquake.
- [56] Wikipedia. https://en.wikipedia.org/wiki/2011_Tokohu_earthquake_and_tsunami.
- [57] Wikipedia. https://en.wikipedia.org/wiki/2017_Chiapas_earthquake.
- [58] Wikipedia. https://en.wikipedia.org/wiki/2019_Ridgecrest_earthquakes.
- [59] Wikipedia. https://en.wikipedia.org/wiki/2022_Taitung_earthquakes.
- [60] Wikipedia. https://en.wikipedia.org/wiki/2023_Turkey%E2%80%93Syria_earthquake.
- [61] Wikipedia. https://en.wikipedia.org/wiki/Tempi_train_crash.
- [62] HistoryOnTheNet, "The 1906 san francisco earthquake and fire." <https://www.historyonthenet.com/authentichistory/1898-1913/5-techlimits/3-sanfrancisco/index.html>, 2012.
- [63] A. Manno. <https://www.thedailybeast.com/the-fbi-followed-marilyn-monroe-for-years-at-the-height-of-mccarthyism-and-came-up-with-nothing>, 2022.
- [64] A. Press. <https://www.politico.com/story/2012/12/marilyn-monroe-fbi-files-reveal-communist-leaning-acquaintances-085570>, 2012.
- [65] P. Carlson. <https://www.smithsonianmag.com/history/nikita-khrushchev-goes-to-hollywood-30668979/>, 2009.
- [66] P. Carlson. <https://www.historynet.com/nikita-khrushchev-ogles-marilyn-monroe/>, 2017.
- [67] Youtube, "Cubans travel to haiti searching for shopping bargains." <https://www.youtube.com/watch?v=oQR7VidXBA4>, 2018.
- [68] Wikipedia. <https://en.wikipedia.org/wiki/Metro-2>.
- [69] National-Geographic. <https://www.nationalgeographic.com/environment/article/arctic-permafrost-is-thawing-it-could-speed-up-climate-change-feature>.
- [70] Nature. <https://www.nature.com/articles/d41586-019-01313-4>.
- [71] The-Siberian-Times. <https://siberiantimes.com/other/others/news/giant-new-50-metre-deep-crater-opens-up-in-arctic-tundra/>.

[72] NEWSGPT. <https://newsgpt.ai/2023/07/23/russias-gateway-to-the-underworld-drone-reveals-worlds-largest-permafrost-crater/>.